The Company of Biologists

RESEARCH ARTICLE

Evidence for spatial vision in *Chiton tuberculatus*, a chiton with eyespots

Alexandra C. N. Kingston*, Daniel R. Chappell* and Daniel I. Speiser‡

ABSTRACT

To better understand relationships between the structures and functions of the distributed visual systems of chitons, we compare how morphological differences between the light-sensing structures of these animals relate to their visually guided behaviors. All chitons have sensory organs – termed aesthetes – embedded within their protective shell plates. In some species, the aesthetes are interspersed with small, image-forming eyes. In other species, the aesthetes are paired with pigmented eyespots. Previously, we compared the visually influenced behaviors of chitons with aesthetes to those of chitons with both aesthetes and eyes. Here, we characterize the visually influenced behaviors of chitons with aesthetes and eyespots. We find that chitons with eyespots engage in behaviors consistent with spatial vision, but appear to use spatial vision for different tasks than chitons with eyes. Unlike chitons with eyes, *Chiton tuberculatus* and *C. marmoratus* fail to distinguish between sudden appearances of overhead objects and equivalent, uniform changes in light levels. We also find that *C. tuberculatus* orients to static objects with angular sizes as small as 10 deg. Thus, *C. tuberculatus* demonstrates spatial resolution that is at least as fine as that demonstrated by chitons with eyes. The eyespots of *Chiton* are smaller and more numerous than the eyes found in other chitons and they are separated by angles of <0.5 deg, suggesting that the light-influenced behaviors of *Chiton* may be more accurately predicted by the network properties of their distributed visual system than by the structural properties of their individual light-detecting organs.

KEY WORDS: Mollusc, Visual ecology, Eye evolution, Orientation, Comparative morphology

INTRODUCTION

A diverse set of invertebrates gather spatial information about light using tens to hundreds to thousands of separate light-detecting organs distributed broadly across their bodies. Examples of these distributed visual systems may be found in taxa that include: cnidarians such as box jellyfish (Nilsson et al., 2005); echinoderms such as brittle stars (Sumner-Rooney et al., 2018), sea stars (Garm and Nilsson, 2014) and sea urchins (Blevins and Johnsen, 2004); annelids such as the tube-dwelling sabellids (Bok et al., 2016) and serpulids (Bok et al., 2017); and molluscs such as ark clams (Nilsson, 1994), giant clams (Wilkens, 1986), scallops (Land, 1965) and chitons (Speiser et al., 2011). Many recent studies have focused

on the optical properties (e.g. Li et al., 2015; Palmer et al., 2017) or molecular components (e.g. Ullrich-Lüter et al., 2011; Pairett and Serb, 2013) of individual eyes from distributed visual systems. Despite these advances, many questions remain regarding how structural differences between distributed visual systems contribute to differences in function. For example, do animals with distributed visual systems gather spatial information within or between their separate light-detecting organs?; and with what types of visually influenced behaviors are these distributed visual systems associated?

To better understand relationships between the structural and functional characteristics of distributed visual systems, we studied how morphological differences between the light-sensing structures of chitons (Mollusca; Polyplacophora) contribute to differences in their visually guided behaviors. Chitons are common to many rocky, intertidal, marine habitats and are protected by eight overlapping shell plates made of aragonite ($CaCO_3$). A variety of sensory organs are embedded within the porous outer (tegmental) layer of these shell plates. In all chitons, these include bundles of unpigmented sensory cells termed aesthetes (Moseley, 1885). These include larger aesthetes that are termed megalaesthetes and the numerous, finer aesthetes that branch from them that are termed microaesthetes (Eernisse and Reynolds, 1994). In some chitons – including species in the subfamilies Acanthopleurinae (Nowikoff, 1907) and Toniciinae (Boyle, 1969), as well as those in the enigmatic genus *Schizochiton* (Moseley, 1885) – the megalaesthetes are interspersed with small eyes. In the eyed chiton *Acanthopleura granulata*, each eye has a lens made of aragonite that focuses light onto a pigment-backed retina (Speiser et al., 2011; Li et al., 2015). In other chitons, including species in the subfamily Chitoninae (Nowikoff, 1909; Haas and Kriesten, 1978) and genus *Callochiton* (Baxter et al., 1990), each megalaesthete is attached to an eyespot composed of pigmented photoreceptors. The eyes of *A. granulata* are ~80 µm in diameter and have retinas with ~100 photoreceptors, making them larger than the eyespots of *Chiton tuberculatus* which are ~35 µm in diameter and consist of clusters of ~20 photoreceptors (A.C.N.K. and D.I.S., unpublished). Previous authors have referred to the eyes and eyespots of chitons as extra-pigmented and intra-pigmented aesthetes, respectively, but we have chosen to use more general terms for brevity and clarity.

Chitons demonstrate a variety of light-influenced behaviors, and the behaviors demonstrated by a particular species appear to be associated with the types of sensory organs present in its shell plates. Although the functions of megalaesthetes may vary between species (Baxter et al., 1987), it is likely that these sensory organs contribute to the light-influenced behaviors (e.g. non-visual phototaxis and defensive shadow responses) that are observed across chitons, including those that lack eyespots or eyes (Boyle, 1972; Speiser et al., 2011). The presence of eyes in chitons is associated with spatial vision: species with eyes distinguish between objects and uniform decreases in light levels, a visual ability not

Department of Biological Sciences, University of South Carolina, Columbia, SC 29208, USA.
*These authors contributed equally to this work

‡Author for correspondence (speiser@mailbox.sc.edu)

D.I.S., 0000-0001-6662-3583

demonstrated by eyeless species (Speiser et al., 2011). In contrast to the established link between eyes and spatial vision in chitons, the presence of eyespots has yet to be linked to particular light-influenced behaviors. Intriguingly, observations from the field suggest that *C. tuberculatus* orients to visual cues from its environment, a behavior yet to be reported for other chitons (Arey and Crozier, 1919).

In this paper, we explore the structure and function of eyespots in chitons. To investigate the internal structure of these eyespots, we made epoxy resin casts of the sensory organs embedded in the anterior shell plates of *C. tuberculatus*, *C. marmoratus*, *C. viridis* and *C. squamosus*. To evaluate the external structure of the eyespots, we imaged the surfaces of shell plates from *C. tuberculatus* and *C. marmoratus* using scanning electron microscopy (SEM). Next, we measured the angular separation between the eyespots of *C. tuberculatus* and *C. marmoratus* to model how the visual systems of these chitons might perform if their eyespots function in a manner analogous to the ommatidia of dispersed compound eyes. To investigate how the light-influenced behaviors of *Chiton* compare with those of other chitons, we conducted two separate behavioral experiments: the first tested whether *C. tuberculatus* and *C. marmoratus* distinguish between the appearances of overhead objects and equivalent, uniform decreases in light levels; the second tested whether the orientation or displacement of

C. tuberculatus is influenced by the presence of static objects in their lateral field of view.

MATERIALS AND METHODS
Collecting and preparing specimens of *Chiton*
Under an Indigenous Species Research, Retention, and Export Permit (DFW16025U), we collected four species of *Chiton* from rocky shores on the island of St Thomas, United States Virgin Islands: *C. tuberculatus* Linnaeus 1758 (Fig. 1A) from Brewers Bay (18.34°N, 64.97°W) and Bordeaux Bay (18.36°N, 65.01°W); *C. marmoratus* Gmelin 1791 (Fig. 1B) and *C. squamosus* Linnaeus 1764 (Fig. 1C) from Mandahl Bay (18.36°N, 64.89°W); and *C. viridis* Spengler 1797 (Fig. 1D) from Bolongo Bay (18.31°N, 64.89°W). Following collection, we transported animals to the University of the Virgin Island's MacLean Marine Science Center, where we kept them in a shaded outdoor flow-through sea table supplied with natural seawater (NSW) from Brewers Bay. We used animals for our behavioral experiments within 7 days of collection. To preserve specimens of *C. tuberculatus* and *C. marmoratus* for later morphological examinations, we fixed whole animals overnight at 4°C in 4% paraformaldehyde in NSW that had been passed through a 0.22 µm syringe filter. We washed fixed specimens three times for 5 min each in filtered NSW and stored them in NSW at 4°C until use. We also preserved specimens of
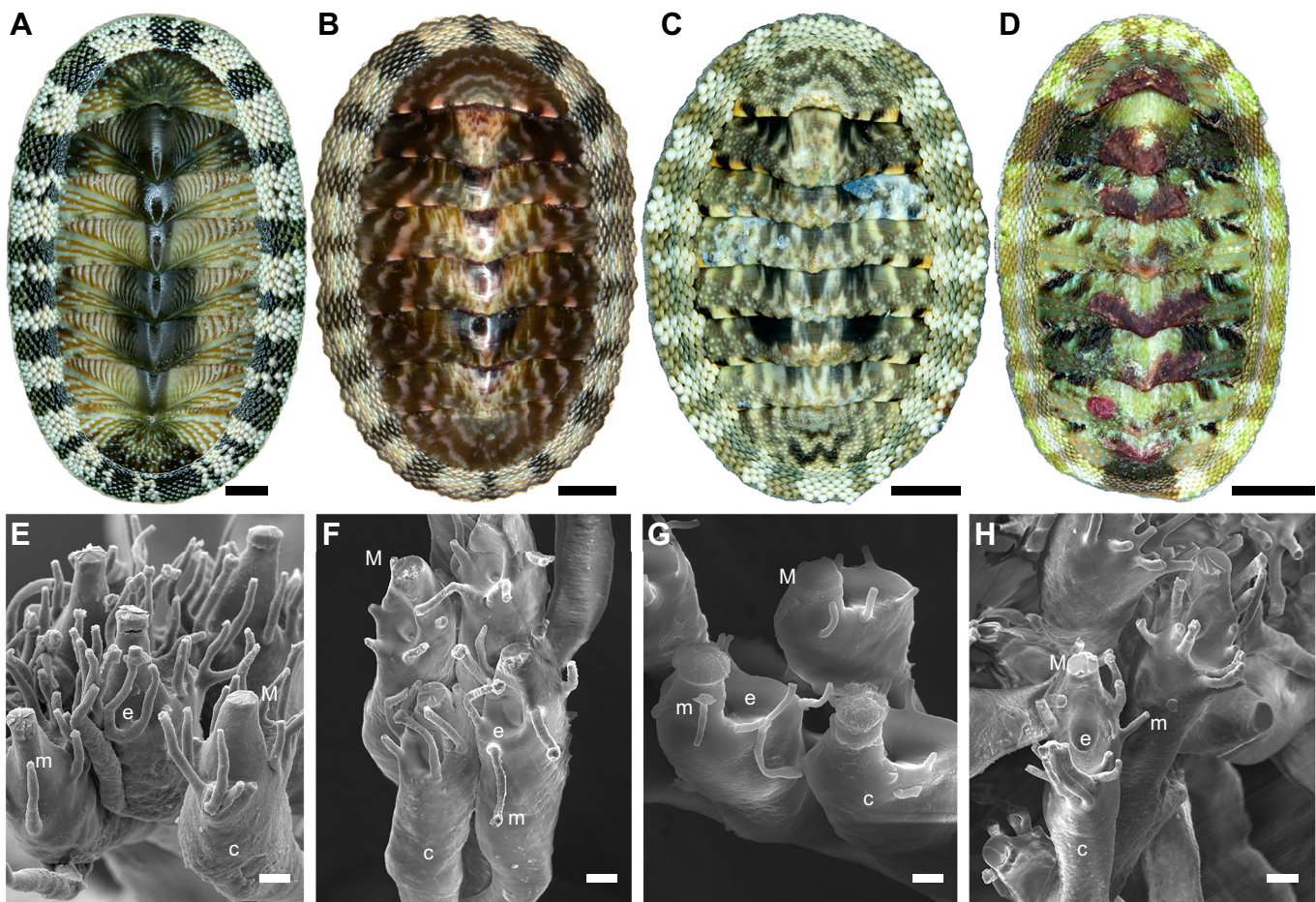

Fig. 1. Morphologies of the sensory complexes from four species of *Chiton*. The species included in this study were *C. tuberculatus* (A), *C. marmoratus* (B), *C. squamosus* (C) and *C. viridis* (D). We compared the sensory complexes of these species using SEM to image epoxy resin casts of shell plates from *C. tuberculatus* (E), *C. marmoratus* (F), *C. squamosus* (G) and *C. viridis* (H). c, central canal; e, eyespot; M, megalaesthete; m, microaesthete. Scale bars in A–D, 1 cm. Scale bars in E–H: 10 µm.

C. tuberculatus, *C. marmoratus*, *C. squamosus* and *C. viridis* in 100% ethanol and stored them at −20°C until use.

Examining the morphology of the sensory structures of *Chiton*

To investigate the internal morphology of the eyespots of chitons, we made epoxy resin casts of the canals associated with the sensory organs embedded in the shell plates of *C. tuberculatus*, *C. marmoratus*, *C. squamosus* and *C. viridis* (following methods described in Fernandez et al., 2007). To make these casts we removed anterior shell plates from ethanol-preserved specimens, soaked these plates in bleach for 24 h, and then embedded them in epoxy resin from an Embed-812 kit (Electron Microscopy Sciences, Hatfield, PA, USA). We mixed components from the kit in the following proportions: 44.1% Embed 812 embedding resin, 35.3% dodecenyl succinic anhydride (DDSA), 17.6% nadic methyl anhydride (NMA) and 2.9% 2,4,6-Tris(dimethylaminomethyl)phenol (DMP-30). During the embedding process, we placed the samples under a vacuum in a desiccating chamber for 1–3 h to facilitate the infiltration of the epoxy resin into the canal structures. We cured the epoxy resin blocks in an oven held at 60°C for 24 h and then trimmed the blocks using a rotary hand tool so that the shell plates were exposed on all sides. Next, we placed the blocks in 10% HCl for 24–48 h to dissolve the shell plates. Once the plates dissolved, we rinsed the blocks in dH₂O, split them into dorsal and ventral halves, and applied a coat of gold to each half using a Denton Desk 2 Sputter Coater (Denton Vacuum, Moorestown, NJ, USA). Finally, we imaged the gold-coated casts with a Tescan Vega 3 SBU with an accelerating voltage of 10 kV (Tescan, Warrendale, PA, USA). To evaluate whether the eyespots of chitons are associated with external light-focusing structures, we used the same equipment described above to image the dorsal surfaces of anterior shell plates from *C. tuberculatus* and *C. marmoratus*. Prior to imaging, we dehydrated these shell plates in ethanol, allowed them to air dry, and applied two coats of gold.

Modeling visual acuity from the distribution of eyespots in *Chiton*

We modeled the performance of the visual system of *Chiton* as if it is organized as an apposition compound eye in which the eyespots function as ommatidia. The angular resolution (Δϕ) of an apposition compound eye is determined by the acceptance angles of its ommatidia (Δρ). However, the angular separation between neighboring ommatidia (Δϕ) is often used as a proxy for angular resolution because in many apposition compound eyes Δρ and Δϕ are similar (Land and Nilsson, 2002; Cronin et al., 2014). Although we cannot assume that Δρ and Δϕ are similar for the visual system of *Chiton*, we calculated Δϕ to get a sense for the best-case scenario for angular resolution in these animals. To calculate Δϕ for *C. tuberculatus* and *C. marmoratus*, we took individual anterior shell plates and divided the angular changes per unit length of their two principal axes of curvature (margin–apex and lateral) by their linear densities of eyespots. We calculated Δϕ for eyespots along the anterior margins of these plates to standardize our approach between samples and because the eyespots of *Chiton* tend to be the most numerous on the anterior plates.

To measure the two principal axes of curvature of the anterior shell plates of *C. tuberculatus* and *C. marmoratus*, we removed a single anterior plate from one ethanol-preserved specimen of each species and photographed these plates using a Nikon D5000 camera mounted to a Leica S6 D Stereozoom microscope. We calibrated the camera set-up using a stage micrometer. We photographed each

shell plate twice: once with the plane of the margin–apex curvature orthogonal to the view of the camera and once with the plane of the lateral curvature orthogonal to the view of the camera. Next, we measured the area density of eyespots on these shell plates by decalcifying the plates in 0.5 mol l⁻¹ EDTA (pH 8.0) for ~48 h on a rocker at room temperature, mounting the remaining soft tissue on slides using Fluormount-G (Southern Biotech, Birmingham, AL, USA), and imaging the tissue using the camera set-up described above. We took all of our measurements with FIJI (Schindelin et al., 2012), using the Kappa plugin (Bechstedt et al., 2014) to calculate the radii of curvature of the shell plates.

Measuring defensive responses of *Chiton* to changes in the overhead light field

Chitons – including those of genus *Chiton* – tend to display a defensive shadow response in which they lower their thick, armored mantle (or 'girdle') down to their substrate when light levels decrease suddenly (Arey and Crozier, 1919; Boyle, 1972). Previously, we used behavioral experiments involving these defensive responses to demonstrate that the eyed chiton *Acanthopleura granulata* distinguishes between the sudden appearances of overhead objects and equivalent, uniform changes in the overhead light field (Speiser et al., 2011). Here, we repeated these experiments with *C. tuberculatus* and *C. marmoratus* to ask if these animals, like *A. granulata*, demonstrate defensive behaviors consistent with spatial vision.

We conducted these behavioral trials from 30 June to 4 July 2016 between the hours of 09:00 and 23:00. We began trials by filling a clear plastic 10×10×10 cm cube (AMAC Plastic Products, Sonoma County, CA, USA) to a depth of 5 cm with NSW. Into these cubes we placed a smooth piece of 10×10×0.5 cm slate that had been kept in the same outdoor sea table as the test animals and then placed a single chiton onto the middle of the piece of slate. We positioned the plastic cube – containing both slate and chiton – inside a frame built out of strips of slotted angle and set an LCD monitor (model E1913Sf; Dell Inc., Round Rock, TX, USA) face down on the top of the frame so that the surface of the screen was 20 cm above the test animal. We observed and recorded the behavior of test animals using two Logitech HD C615 webcams that were mounted on tripods, positioned on adjacent sides of the plastic cube, and connected to a laptop computer. After positioning the plastic cube inside the slotted angle frame, we covered our set-up with a double layer of black felt.

For these behavioral trials, we presented chitons with eight different PowerPoint slides that were displayed on the monitor positioned overhead and re-ordered randomly for each test animal. Each of the slides started with a white background, displayed a stimulus for 3 s, and then returned to a white background. In four of the slides, a single black circular target was displayed. As measured from the initial position of the test animals, these targets had angular sizes of 1, 3, 9 or 27 deg and their appearances caused decreases in irradiance of 0, 1, 3 and 17%, respectively. Each of these slides was paired with a uniform gray slide whose appearance caused an equivalent decrease in irradiance; here, note that the slide that matched the 1 deg target was a uniform white (Table 1). We measured the absolute irradiance (from 400 to 700 nm) of the white background and the eight slides using a spectrometer system from Ocean Optics (Dunedin, FL, USA) that included a Flame-S-VIS-NIR-ES spectrometer, a QP400-1-UV-VIS optical fiber, and a CC-3 cosine-corrector. We calibrated the absolute spectral response of our system using a HL-3P-CAL calibrated Vis-NIR light source and operated the spectrometer using Ocean View software.

Table 1. Absolute irradiance of stimuli used in overhead trials

Slide	Irradiance ($\times 10^{14}$ photons cm^{-2} s^{-1})	Change in light level (%)
White	2.38	0
1 deg target	2.38	0
Gray slide matching 1 deg target	2.38	0
3 deg target	2.37	1
Gray slide matching 3 deg target	2.37	1
9 deg target	2.32	3
Gray slide matching 9 deg target	2.32	3
27 deg target	1.98	17
Gray slide matching 27 deg target	1.98	17

Here, we report measures of absolute irradiance (integrated from 400 to 700 nm) for each stimulus used to measure the defensive responses of *Chiton tuberculatus* and *C. marmoratus* to changes in the overhead light field.

Before a behavioral trial began, we waited for a chiton to lift a portion of its girdle and begin crawling along the slate substrate. Acclimation by chitons to the behavioral arena usually took less than 2 min. We only recorded a chiton's response to a stimulus if the responses occurred within 3 s of the stimulus being presented. We scored a response as 'partial' if a chiton lowered its girdle partially and 'total' if a chiton lowered its girdle completely and ceased crawling. If a chiton did not respond to a stimulus, we presented the next slide after a several second delay. If a chiton did respond to a stimulus, we presented a new slide after it resumed crawling. If a chiton crawled up the walls of the plastic cube, we repositioned it back onto the slate and provided an additional acclimation period before resuming the trial.

Two viewers, blind to the stimuli being presented, simultaneously scored the video recordings of these behavioral trials in real time. We used the response rate of chitons to the appearance of the uniform white slide (which produced a 0% change in irradiance) as an estimate of the rate at which chitons displayed defensive responses spontaneously. We then used Fisher's exact test to compare this rate of spontaneous response to the response rates of chitons to each of the visible stimuli (i.e. the black circular targets and the uniform gray screens). In these statistical tests, we did not distinguish between partial and total responses by chitons.

Measuring the orientation and displacement of *Chiton* in response to static visual stimuli

To test if the movements of *Chiton tuberculatus* may be influenced by the presence of visible objects in their environment, we conducted behavioral trials to see how animals responded to dark, static, circular targets presented in their lateral fields of view. We conducted trials from 30 June to 1 July 2016 between the hours of 9:00 and 19:00 under fluorescent room lights. For a testing arena, we used a white plastic bucket with a tight-fitting white plastic lid that diffused the room light (Fig. S1). Using the spectrometer system described above, we verified that the down-welling and horizontal light fields were uniform within the bucket. A Logitech HD Webcam C615 viewed the inside of the behavioral arena through a small hole bored into the center of the lid. As targets, we fastened circles of black felt to the inside of the bucket so that their centers were 3.8 cm from the bottom. To minimize the influence of non-visual sensory cues, such as magnetoreception (Sumner-Rooney et al., 2014), we ran 32 trials in a randomized order that combined all possible combinations of target size (angular sizes of 10 or 30 deg as measured from the middle of the bucket), target position (0, 90, 180, 270 deg), and initial orientation of the test animal (0, 90, 180, 270 deg). Separate animals were used for each of the 32 trials and each

trial included a single chiton and a single target. To begin a trial, we placed a chiton inside the testing arena, secured the lid on the bucket, and recorded photos every 10 s for 10 min using the webcam. After each trial, we cleaned and dried the bucket to discourage test animals from following trails left behind by previous animals.

To analyse the results of these behavioral trials, we imported our images from time-lapse photography into FIJI (Schindelin et al., 2012) and used the Trackmate plugin (Tinevez et al., 2017) to acquire the orientation and displacement of our test animals at every time point. We then calculated the mean orientation and displacement of each animal relative to the target (which we set at 0 deg). We used mean values because we had different numbers of discrete time points for each trial due to animals taking different amounts of time to reach the edge of the behavioral arena. We excluded positional data recorded after animals reached the edge of the arena (which happened in 12 out of our 32 trials) because chitons prefer crawling along edges rather than traveling across flat surfaces (i.e. they exhibit thigmotaxis; Sumner-Rooney et al., 2014).

We performed statistical analyses on our data using two separate software packages. In both cases, we analysed separately the orientation and displacement of chitons for each of the target sizes (10 and 30 deg). As our first approach, we used a model selection procedure implemented in 'CircMLE' (Fitak and Johnsen, 2017) in R (https://cran.r-project.org/web/packages/CircMLE/index.html). For a given data set, CircMLE calculates the maximum likelihood of the 10 models of animal orientation proposed by Schnute and Groot (1992) and compares them using the Akaike information criterion (AIC; Akaike, 1973) or corrected AIC (AICc; Hurvich and Tsai, 1989) tests. The models of animal orientation evaluated by CircMLE include: a uniform model (M1); three unimodal models (M2A, M2B and M2C); four axial bimodal models (M3A, M3B, M4A and M4B): and two non-axial bimodal models (M5A and M5B). We used AICc for model comparison due to our small sample sizes (N=16 for both target sizes) and we defined good support as AICc scores of <2.00 (Burnham and Anderson, 2004; Burnham et al., 2011).

As our second approach, we used the 'circular' package (version 0.4-93; https://CRAN.R-project.org/package=circular) in R to test for directionality using Rayleigh tests. For these tests, our null hypotheses were that test animals demonstrated uniform distributions of orientation and displacement. Our alternate hypotheses were that test animals oriented towards or moved towards the positions of the targets (i.e. unimodal distributions of orientation and displacement) or that test animals tended to orient or move directly towards or directly away from the targets (i.e. axial distributions of orientation and displacement). For all of our Rayleigh tests, we set the threshold for significance at 5% and specified a mean direction (ϕ) of 0 deg. To test for axial responses, we doubled the headings of each data point (Batschelet, 1981).

RESULTS

The sensory complexes of *Chiton* are similar morphologically

The megalaesthetes, microaesthetes and eyespots of *C. tuberculatus* (Fig. 1A,E), *C. marmoratus* (Fig. 1B,F), *C. squamosus* (Fig. 1C,G), and *C. viridis* (Fig. 1D,H) form complexes that are morphologically similar. Epoxy resin casts of the shell plates of these four species reveal complexes of sensory organs that consist, proximally, of a central canal (~30 μm in diameter) and, distally, of a megalaesthete (~15 μm in diameter) and an attached structure (~45 μm in

diameter) with a depression that is associated with the location of the eyespot (Fig. 1E–H). Similar to past observations for *C. marmoratus*, we found that the side of each depression nearest its neighboring megalaesthete deepens sharply into a pit (termed Linsenzapfen – or 'lens pin' – by Haas and Kriesten, 1978). Numerous microaesthetes (∼6 µm in diameter) branch from the central canals of the sensory complexes in all four species of *Chiton*. The number of microaesthetes per complex vary between the species surveyed: *C. tuberculatus* and *C. viridis* had ∼14, whereas *C. marmoratus* and *C. squamosus* had ∼6.

External morphology of the shell plates of *Chiton*

The shell plates of *C. tuberculatus* and *C. marmoratus* differ in external morphology in ways that might be relevant to the detection of light by the eyespots of these two species. The eyespots of *C. tuberculatus* are associated with overlying shell material that is transparent and convex. Light microscopy indicates that the shell material overlying the eyespots is transparent: pigment associated with individual eyespots is visible through the outer surface of the shell. Between the smooth, elongate, somewhat irregularly sized and spaced tubercles for which *C. tuberculatus* is named, our SEM images reveal smaller, regularly sized and spaced bumps packed at a density of ∼400 mm^{-2} (Fig. 2A). Decalcified shell plates from *C. tuberculatus* indicate that the sizes, positions and packing densities of these bumps correspond to the sizes, positions and packing densities of the underlying sensory complexes (Fig. 2B).

The bumps associated with the sensory complexes of *C. tuberculatus* are elongated along their anterior–posterior axes, having axial and lateral diameters of 70±5 and 35±3 µm, respectively (means±s.d.; *N*=12 in both cases). The posterior sides of each of these bumps contain a single perforated apical cap; these caps have diameters of 14±1 µm (*N*=12) and each is associated with an underlying megalaesthete. Smaller subsidiary caps are also abundant; these have diameters of 4±1 µm (*N*=12), outnumber the larger apical caps by a margin of ∼9:1, and are associated with underlying microaesthetes. The anterior end of each bump is devoid of apical or subsidiary caps. These cap-free zones are elongated
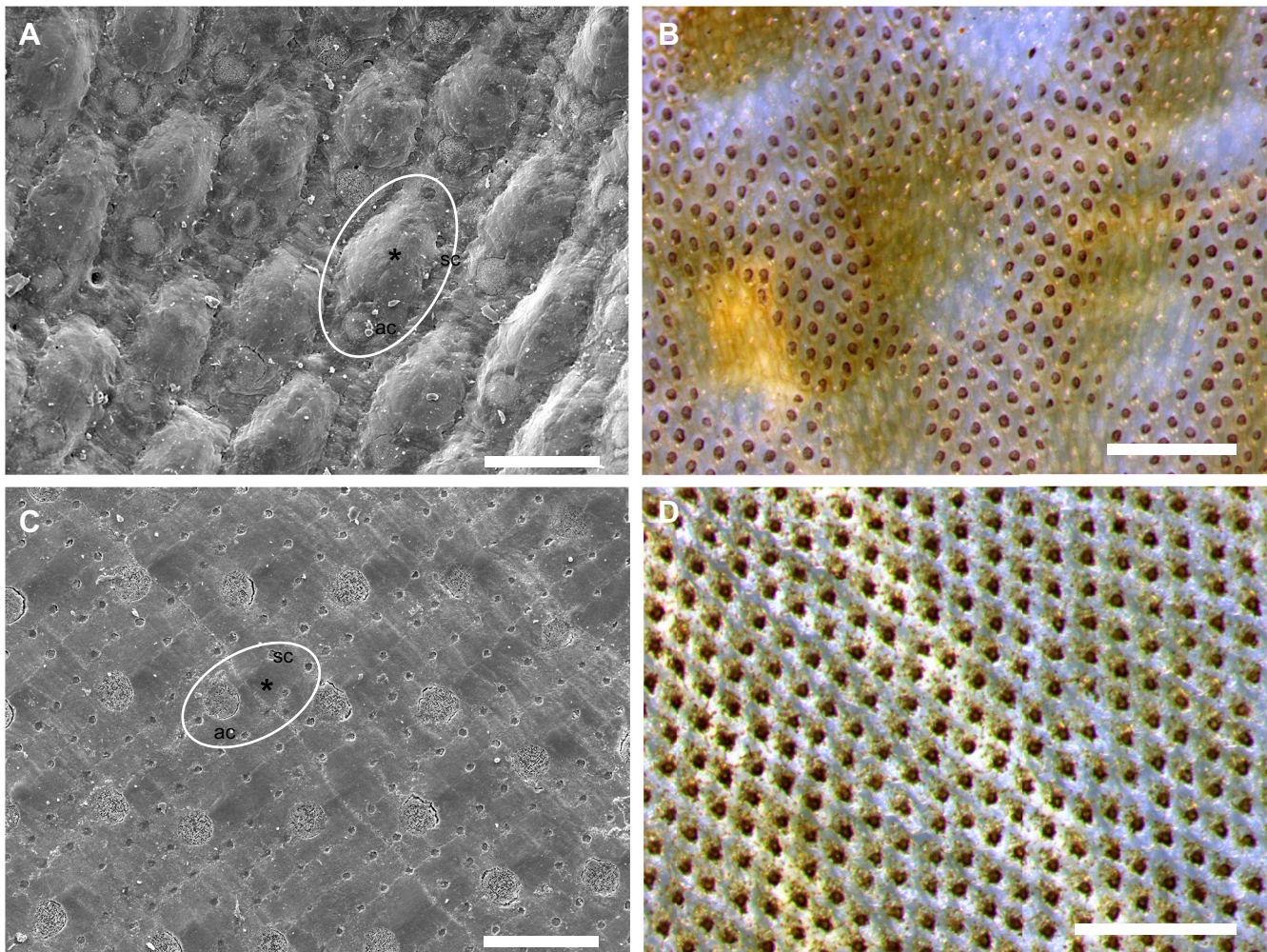

Fig. 2. External and internal shell plate morphology of *C. tuberculatus* and *C. marmoratus*. SEM image of the surface of an anterior shell plate from *C. tuberculatus* (A) and a light microscope image of a decalcified anterior shell plate from the same species (B). In B, the regions of the shell plate that lack pigmented eyespots correspond to the positions of tubercles on the intact sample. Corresponding images are provided for the external (C) and internal (D) morphology of anterior shell plates from *C. marmoratus* (a species that lacks tubercles). ac, apical caps associated with megalaesthetes; sc, subsidiary caps associated with microaesthetes; *transparent region of shell plate; white circle, the shell surface area corresponding to one sensory complex. Scale bars in A and C: 50 µm. Scale bars in B and D: 250 µm.

along their anterior–posterior axes, having axial and lateral diameters of 40±3 and 31±3 µm, respectively (N=12 in both cases). Curiously, the tubercles of *C. tuberculatus* contain apical caps and subsidiary caps, but lack both pigmented eyespots and the smaller surface convexities that are abundant in other regions of the shell plates.

The eyespots of *C. marmoratus* are not associated with external shell features consistent with a lens. As in *C. tuberculatus*, light microscopy suggests that transparent shell material overlies the eyespots of *C. marmoratus*. However, in *C. marmoratus*, these transparent regions appear to be flush with the surface of the shell plate (Fig. 2C). Based on images of decalcified shell plates from *C. marmoratus*, the sizes, positions and packing densities of the transparent regions of shell plate correspond to the sizes, positions and packing densities of the underlying eyespots (Fig. 2D).

From our SEM images for *C. marmoratus*, we identified perforated apical caps associated with the megalaesthetes. These had diameters of 15±1 µm (N=15) and were packed at a density of ~400 mm^{-2}. Smaller subsidiary caps with diameters of 3±1 µm (n=15) surround the larger apical caps; these caps are associated with microaesthetes and are, accordingly, more numerous than the larger apical caps at a ratio of ~8:1. Each megalaesthete is also associated with an adjacent region of shell devoid of apical or subsidiary caps. These cap-free zones are anterior to their adjacent apical caps and are slightly elongated along their anterior–posterior axes, having axial and lateral diameters of 18±4 and 16±2 µm, respectively (N=15 in both cases).

The eyespots of *Chiton* have angular separations of less than 0.5 deg

Eyespots on the anterior shell plates of *C. tuberculatus* and *C. marmoratus* are separated by angles of 0.5 deg or less. The anterior shell plates from the specimens of *C. tuberculatus* and *C. marmoratus* that we surveyed had margin–apex radii of curvature of 8.0 and 6.9 mm, respectively, and lateral radii of curvature of 14.5 and 13.2 mm, respectively. Once we decalcified these shell plates, we identified the eyespots by their dark pigmentation (Fig. 2B,D). In both species, the central anterior margins of the anterior shell plates are packed with ~400 eyespots mm^{-2}.

Chiton marmoratus and *C. tuberculatus* did not distinguish between the appearances of objects and uniform changes in the overhead light field

We found that *C. tuberculatus* (N=32) and *C. marmoratus* (N=32) respond to changes in their overhead light field (usually within 1 s), but do not distinguish between the appearances of objects and equivalent, uniform changes in light levels (shadows) (Fig. 3). Using Fisher's exact test, we found that the rates at which *C. tuberculatus* responded defensively (Fig. 3A) to the 27 deg target (81% of individuals responding; P=6.89×10^{-11}) and the 17% decrease in down-welling irradiance (94%; P=1.78×10^{-14}) differed significantly from their response rate to the uniform white slide (representing a 0% decrease in down-welling irradiance) that we used as a control stimulus (3%). Likewise, the response rates of *C. marmoratus* (Fig. 3B) to the 27 deg target (100%; P=3.60×10^{-17}) and the 17% decrease in down-welling irradiance (100%; P=3.60×10^{-17}) differed significantly from their response rate to the control stimulus (3%). Neither species of *Chiton* appeared to distinguish between the 27 deg target and the uniform gray screen that caused a 17% decrease in irradiance (*C. tuberculatus*, P=0.25; *C. marmoratus*, P=1).

We also found that *C. tuberculatus* and *C. marmoratus* did not distinguish between the control stimulus and the appearances of targets with angular sizes of <27 deg or uniform gray screens that caused decreases in down-welling irradiance of <17%. Again using Fisher's exact test, we found that the response rates of *C. tuberculatus* (Fig. 3A) to the 1 deg (3%; P=1), 3 deg (3%; P=1) and 9 deg (9%; P=0.61) targets and the uniform 1% (9%; P=0.61) and 3% (12%; P=0.35) decreases in irradiance did not differ significantly from their response rates to the uniform white slide that we used as a control stimulus (3%). Similarly, the response rates of *C. marmoratus* (Fig. 3B) to the 1 deg (6%; P=1), 3 deg (0%; P=1) and 9 deg (6%; P=1) targets and the uniform 1% (0%; P=1) and 3% (12%; P=0.35) decreases in irradiance did not differ significantly from their response rates to the control (3%).

Chiton tuberculatus orients to visual landmarks

Our behavioral experiments indicate that *C. tuberculatus* orients to dark, static, circular targets with angular sizes of 10 or 30 deg that
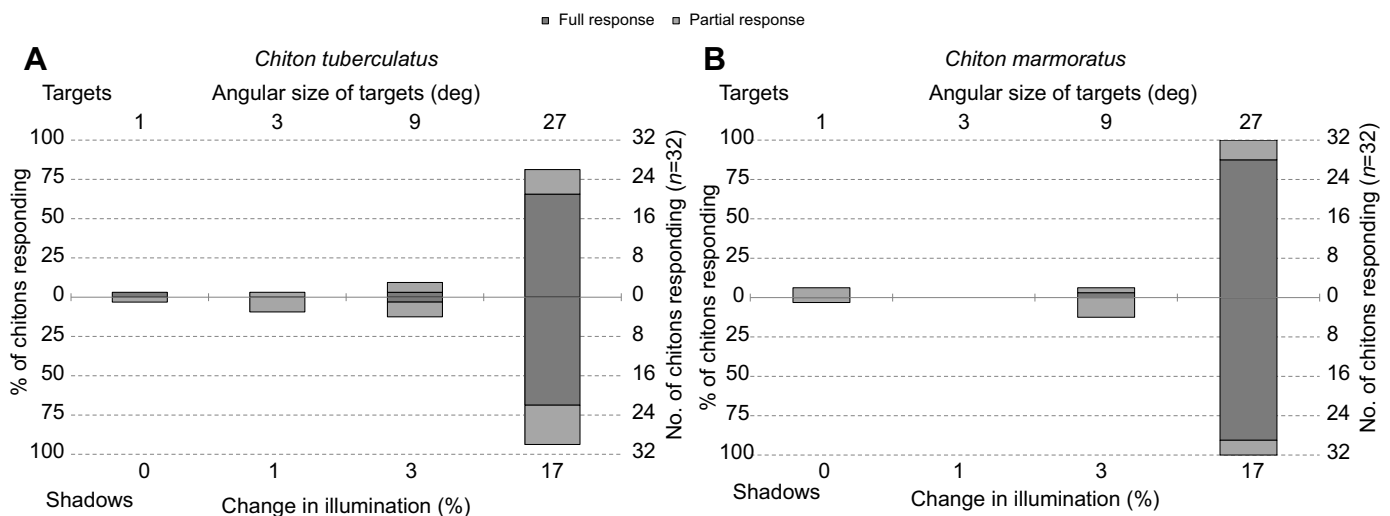
■ Full response   ■ Partial response

Fig. 3. The defensive responses of *Chiton tuberculatus* and *Chiton marmoratus* to changes in their overhead light field. We compared the defensive responses of chitons to the sudden appearances of overhead objects ('targets') to the responses of these animals to equivalent, uniform changes in the overhead light field ('shadows'). We found that *C. tuberculatus* and *C. marmoratus* respond to changes in light levels, but do not distinguish between the appearances of targets and equivalent, uniform changes in light levels.

Table 2. Orientation and displacement of *Chiton tuberculatus* to static visual stimuli

Behavior		Displacement		Orientation	
Target size (deg)		10	30	10	30
Rayleigh test	N	16	16	16	16
	P	0.48	0.06	0.005	0.03
Model ΔAICc	M1	**0.00*(0.66)**	**0.00*(0.48)**	4.96 (0.07)	**0.08 (0.26)**
	M2A	3.86 (0.09)	4.04 (0.06)	7.04 (0.02)	4.07 (0.04)
	M2B	4.04 (0.08)	4.00 (0.07)	2.64 (0.14)	2.39 (0.08)
	M2C	8.23 (0.01)	6.22 (0.02)	7.83 (0.00)	2.96 (0.06)
	M3A	4.03 (0.09)	**1.55 (0.23)**	**0.00*(0.50)**	**0.00*(0.27)**
	M3B	7.10 (0.02)	4.42 (0.05)	**1.85 (0.12)**	**1.80 (0.11)**
	M4A	7.10 (0.02)	4.35 (0.06)	**2.00 (0.11)**	2.21 (0.09)
	M4B	10.59 (0.00)	7.97 (0.01)	3.85 (0.02)	2.88 (0.07)
	M5A	9.45 (0.01)	7.23 (0.01)	6.72 (0.00)	7.50 (0.01)
	M5B	13.80 (0.00)	11.58 (0.00)	**1.52 (0.02)**	7.11 (0.01)

For our Rayleigh tests of axial orientation and displacement by *C. tuberculatus*, we show sample size (*N*) and *P*-value (*P*) for trials involving targets with angular sizes of 10 or 30 deg. For the model selection tests, we show ΔAICc (probabilities in parentheses) for the 10 separate orientation models under consideration. Models with ΔAICc<2 are shown in bold, with the best models indicated by an asterisk.

are presented in its lateral field of view (Table 2). Using a model selection procedure (AICc), we found that the orientation of *C. tuberculatus* to the 10 deg target was best explained by an axial bimodal model (M3A, ΔAICc=0.00; Fig. 4A). We also found good support for two other axial bimodal models (M3B, ΔAICc=1.85; M4A, ΔAICc=2.00) and one nonaxial bimodal model (M5B, ΔAICc=1.52). The mean directions of the first and second distributions for these models were: M3A, ϕ_1=184 deg and ϕ_2=4 deg; M3B, ϕ_1=187 deg and ϕ_2=7 deg; M4A, ϕ_1=4 deg and ϕ_2=184 deg; and M5B, ϕ_1=20 deg and ϕ_2=168 deg (these distributions

Fig. 4. Orientation and displacement of *Chiton tuberculatus* in response to dark targets. Mean directions (red arrows) and circular histograms in 20 deg bins (gray segments) describing the orientation of *C. tuberculatus* to targets with angular sizes of 10 deg (A) or 30 deg (B) and the displacement of *C. tuberculatus* to the same 10 deg (C) or 30 deg (D) targets. In A and B, we provide the density (dashed line) and mean axial distribution (black arrows) of the best-supported model of orientation (M3A in both cases). We do not show mean axial distribution for C and D, because displacement by *C. tuberculatus* was best described by a uniform distribution (M1) for both the 10 and 30 deg targets.

indicate axial orientation when ϕ_2=ϕ_1±180 deg; Fitak and Johnsen, 2017). In all of these cases, the proportional size of the first distribution (λ) was 0.5. The model weights, or probabilities, for models M3A, M3B, M4A and M5B were 50, 12, 11 and 2%, respectively.

Similarly, we found that the orientation of *C. tuberculatus* to the 30 deg target was best described by an axial bimodal model (M3A, ΔAICc=0.00; Fig. 4B) and was well described by another axial bimodal model (M3B, ΔAICc=1.80). The mean directions of the first and second distributions for these axial bimodal models were: M3A, ϕ_1=349 deg and ϕ_2=169 deg; and M3B, ϕ_1=169 deg and ϕ_2=349 deg. For both of these axial bimodal models, the proportional size of the first distribution (λ) was 0.5. We also received strong support for a model of uniform distribution (M1, ΔAICc=0.08). The probabilities for models M1, M3A and M3B were 26, 27 and 11%, respectively.

Results from our Rayleigh tests (Table 2) were consistent with the results from our model selection procedure: we found that the orientations of *C. tuberculatus* in response to the 10 or 30 deg targets were well described by axial bimodal distributions (*P*<0.05 for both target sizes) and poorly described by unimodal distributions (*P*>0.05 in both cases). Thus, we received consistent support for models indicating that *C. tuberculatus* tended to orient either towards (ϕ=0 deg) or away (ϕ=180 deg) from the 10 and 30 deg targets. However, for the 30 deg target, strong support for a model of uniform distribution (M1) weakens the support for the axial bimodal models.

Chiton tuberculatus did not crawl towards or away from visual landmarks

Although *C. tuberculatus* orient their body axes to static targets, we do not find strong support that they crawl towards or away from these targets (Table 2). We found that the displacement of *C. tuberculatus* in response to either the 10 deg (Fig. 4C) or 30 deg (Fig. 4D) target was best explained by a model of uniform distribution (M1, ΔAICc=0.0). The only other model that was supported by our results was an axial model for the displacement of test animals to the 30 deg target (M3A, ΔAICc=1.55). The mean directions of the modes for this model were 13 and 193 deg and the proportional size of the first distribution was 0.5, suggesting that there was equal displacement by animals towards (0 deg) and away (180 deg) from the 30 deg target. For displacement in response to the 30 deg target, the probabilities for models M1 and M3A were 31 and 23%, respectively.
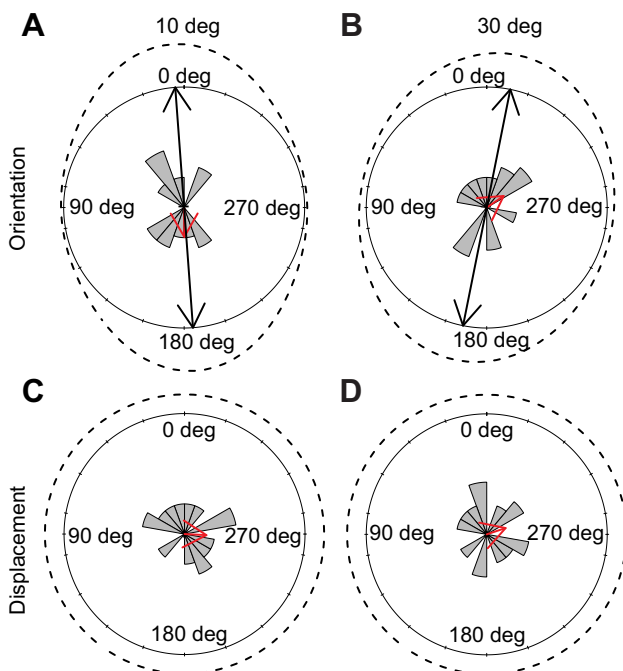
Results from our Rayleigh tests (Table 2) were again consistent with the results from our model selection procedure: *C. tuberculatus* did not demonstrate significant displacement towards either the 10 or 30 deg targets ($P>0.05$ in both cases); they also did not prefer to travel along the axes defined by either target ($P>0.05$ in both cases). Thus, multiple statistical approaches agree that *C. tuberculatus* did not appear to prefer crawling either towards or away from the 10 or 30 deg targets.

DISCUSSION
Structure and function of the visual system of *Chiton*
The shell plates of *C. tuberculatus* and *C. marmoratus* contain ~400 eyespots mm^{-2}. Similar estimates of eyespot density were obtained from viewing external valve characteristics and from viewing the eyespots directly from decalcified shell plates. The eyespots appear to be present at similar densities across the separate shell plates of *C. tuberculatus* and *C. marmoratus* and across individuals of different sizes. Chitons add new shell material and new sensory organs as they grow, so we estimate that adult specimens of *Chiton* can have hundreds to thousands of eyespots distributed across each of their eight shell plates. The eyespots on the anterior shell plates of *C. tuberculatus* and *C. marmoratus* are separated by angles of 0.5 deg or less. Because the shell plates of chitons do not have the same radii of curvature in all directions and change shape as they grow, the angular separations of adjacent eyespots in *Chiton* almost certainly vary between the separate shell plates of any given individual and between the corresponding shell plates of individuals of different sizes.

Our behavioral trials indicate that the distributed visual system of *Chiton* provides an angular resolution of ≤10 deg. However, we do not have direct evidence to evaluate whether *Chiton* gathers spatial information by comparing light input between photoreceptors within the same eyespot (in which case the eyespots should be considered small camera-type eyes) or between the photoreceptors of neighboring eyespots (in which case we would model the eyespots as the ommatidia of a dispersed apposition compound eye). Other possibilities exist that blur the distinctions between camera-type and compound eyes – e.g. the aggregate or schizochroal eyes found in animals such as strepsipteran flies (Buschbeck et al., 1999) and some trilobites (Fordyce and Cronin, 1993) – but we will focus on these two straightforward options as a starting point for deciphering the visual system of *Chiton*.

Whether or not the individual eyespots of *Chiton* function as camera-type eyes depends on their size and their association (or lack thereof) with light-focusing structures such as lenses. Both of these considerations lead us to predict that individual eyespots should provide coarser angular resolution than the eyes found in other species (~10 deg for *A. granulata*; Speiser et al., 2011; Li et al., 2015). First, the eyespots of *C. tuberculatus* are ~35 μm in diameter and consist of ~20 pigmented photoreceptor cells; in comparison, the eyes of *A. granulata* are ~80 μm in diameter and contain well-defined retinas of ~100 photoreceptors (A.C.N.K. and D.I.S., unpublished). Second, the eyes of *A. granulata* are each associated with a transparent lens that focuses light on to the photoreceptors of the retina (Speiser et al., 2011; Li et al., 2015); in comparison, it is unclear whether the eyespots of *Chiton* are associated with similar light-focusing structures. Consistent with observations by Haas and Kriesten (1978) for *C. marmoratus*, we find that the eyespots of *C. tuberculatus* and *C. marmoratus* are overlain with transparent shell material. In *C. tuberculatus*, at least some of these transparent regions are associated with surface convexities that could serve lens-like functions; in comparison, the transparent regions of shell

in *C. marmoratus* are flush with the shell surface. Additional work will be necessary to evaluate whether the transparent structures in the shell plates of *Chiton* help focus light on to underlying photoreceptors.

Due to their smaller size and ambiguous association with light-focusing structures, we find it unlikely that individual eyespots from *Chiton* provide spatial resolution equivalent to that provided by the eyes of species such as *A. granulata*. If so, how can we explain the results of behavioral trials indicating that *C. tuberculatus* and *A. granulata* demonstrate spatial vision with similar angular resolutions (≤10 deg)? One possible explanation is that spatial vision in *C. tuberculatus* may not be limited by the resolving power of its individual eyespots. Thus, it may be more accurate to model spatial vision in *Chiton* as if this animal's numerous, densely packed eyespots are functioning in a manner similar to the ommatidia of an apposition compound eye. We consider this an intriguing possibility because the angular separations between the eyespots of *C. tuberculatus* and *C. marmoratus* ($\Delta\phi<0.5$ deg) are similar to the interommatidial angles measured for the foveal regions of the high-acuity apposition compound eyes of dragonflies (Labhart and Nilsson, 1995). Future work on this matter will focus on calculating the acceptance angles ($\Delta\rho$) of the eyespots of chitons and conducting behavioral experiments that will provide more precise estimates of spatial acuity in these animals.

The visual ecology of *Chiton*
Our behavioral experiments indicate that *C. tuberculatus* orients its body to visual cues. These findings are consistent with field observations suggesting that *C. tuberculatus* may use spatial information about light to help guide them to shaded rock refuges at sunrise after nights of foraging (Crozier, 1921). While engaged in these homing behaviors, *C. tuberculatus* were observed traveling orthogonally to the rays of the rising sun rather than crawling directly away from them, as would be predicted if these animals were demonstrating non-visual negative phototaxis (Crozier, 1921). Eyed chitons (e.g. *Acanthopleura gemmata*) also engage in homing behaviors, but it has been argued that these chitons predominantly use chemosensory cues for navigation rather than vision (Chelazzi et al., 1987, 1990).

The behaviors demonstrated in our trials by *C. tuberculatus* may have been affected by the ambient light conditions in our experimental set-up. Field observations suggest that *C. tuberculatus* seek shaded refuges at dawn under clear skies but continue foraging on foggy or cloudy days (Crozier, 1921). Our behavioral trials involving static visual stimuli were lit by diffuse fluorescent room light, which may have led to conditions too dim to elicit refuge-seeking behavior by *C. tuberculatus*. However, the observed orientation to visual stimuli by *C. tuberculatus* indicates that these animals can detect objects with angular sizes as small as 10 deg, even if they are not motivated to move towards them. Future experiments on refuge-seeking behavior in *C. tuberculatus* and *C. marmoratus* will include a variety of background illumination levels.

The stepwise evolution of eyes in chitons
Do the structural complexities of an animal's light-detecting organs predict the complexities of its light-influenced behaviors? If so, the evolution of vision may be a stepwise process in which the addition of components to light-detecting organs is associated with these organs becoming associated with new, more varied, or more complex behaviors. Across evolutionary time, a sequence of these steps could include: (1) the origin of non-pigmented photoreceptors

useful for monitoring temporal changes in light; (2) the origin of eyespots that preferentially sample light from restricted regions of space through the addition of screening pigment to photoreceptors; and (3) the origin of image-forming eyes through the addition of a focusing mechanism, such as a lens, to an eyespot-like structure (Nilsson, 2009, 2013; Oakley and Speiser, 2015). Transitions between these evolutionary steps tend to be conceived of as gradual (von Salvini-Plawen and Mayr, 1977; Nilsson and Pelger, 1994), but punctuated transitions may be possible as well (Plachetzki and Oakley, 2007).

Consistent with a stepwise model of eye evolution, the eyespots of chitons are more structurally complex than megalaesthetes and less complex than eyes. Furthermore, molecular and morphological approaches to systematics concur that eyespots and eyes are derived characters among chitons (Okusu et al., 2003; Sirenko, 2006). Of particular relevance to the current study, conventional classifications of chitons propose a family Chitonidae that is composed of subfamily Chitoninae, which contains species with eyespots (including those in *Chiton*), along with subfamilies Acanthopleurinae and Toniciinae, both of which contain species with eyes (Sirenko, 2006). Thus, a phylogenetic perspective suggests that within Chitonidae, the eyes found in species from Acanthopleurinae and Toniciinae may have evolved from an ancestral megalaesthete-like sensory organ via an eyespot-like intermediate similar to those observed in species from Chitoninae. However, a phylogenetic perspective does not rule out the possibility that eyespots and eyes evolved separately within Chitonidae.

We find that *C. tuberculatus*, a chiton with eyespots, and *A. granulata*, a chiton with eyes, both demonstrate spatial vision with an angular resolution of ≤10 deg, but our behavioral trials indicate that these two species may use spatial vision for different tasks. Unlike *A. granulata*, neither *C. tuberculatus* nor its congener *C. marmoratus* distinguish between the appearances of objects and equivalent, uniform decreases in light levels. We also observed that *C. tuberculatus* orient their bodies so that their anterior ends tend to face towards or away from dark targets with angular sizes as small as 10 deg, a behavior that has not been reported for any other species of chiton. We conclude that the eyespots of *Chiton* are associated with a novel visual response: the light-influenced behaviors of these chitons are different from those observed previously in either eyeless species or those with eyes. To more thoroughly address whether the eyespots of chitons may be a functional intermediate between megalaesthetes and eyes, we will need to rule out the possibility that static visual cues influence the orientation and displacement of eyed chitons (e.g. *A. granulata*).

Conclusions

Here, we present evidence for spatial vision in *C. tuberculatus*, a chiton with eyespots. We find that chitons with eyespots (e.g. *C. tuberculatus*) and chitons with eyes (e.g. *A. granulata*) may use spatial vision for different tasks, i.e. orientation to static cues versus distinguishing between the appearances of overhead objects and uniform changes in light levels. We also argue that chitons with eyespots may gather spatial information by comparing input between photoreceptors of neighboring light-detecting organs, whereas chitons with eyes may obtain spatial information by comparing input between photoreceptors within the same light-detecting structures. Further work will be necessary to evaluate the degree to which chitons – of any sort – integrate information across their distributed sensory networks.

Thinking about the aesthetes of chitons as components of integrated sensory networks prompts questions regarding how such

networks co-evolve with the neural circuits that process the sensory information they collect. For example, how similar are the neural circuits underlying the visual systems of chitons with eyes and chitons with eyespots? If eyed chitons like *A. granulata* are gathering spatial information within eyes and if chitons with eyespots, such as *Chiton*, are gathering spatial information between eyespots, these chitons might have fundamentally different methods for integrating visual information across their sensory networks. Chitons had long been thought to have simple, aganglionic nervous systems, but recent evidence suggests that their anterior nerve ring ought to be considered a true brain; furthermore, it appears that nervous system organization varies between chiton taxa (Sumner-Rooney and Sigwart, 2018). We hope that our work here highlights the diversity and complexity of sensory systems found across invertebrates – even among those that may at first appear to be 'living rocks' – and encourages a deeper exploration of the neural mechanisms that underlie the processing of spatial information obtained by distributed visual systems.

Author contributions
Conceptualization: A.C.N.K., D.R.C., D.I.S.; Methodology: A.C.N.K., D.R.C., D.I.S.; Software: D.R.C.; Validation: A.C.N.K., D.R.C., D.I.S.; Formal analysis: A.C.N.K., D.R.C., D.I.S.; Investigation: A.C.N.K., D.R.C., D.I.S.; Resources: D.I.S.; Data curation: A.C.N.K., D.R.C., D.I.S.; Writing - original draft: A.C.N.K., D.R.C., D.I.S.; Writing - review & editing: A.C.N.K., D.R.C., D.I.S.; Visualization: A.C.N.K., D.R.C., D.I.S.; Supervision: D.I.S.; Project administration: D.I.S.; Funding acquisition: D.I.S.

Supplementary information
Supplementary information available online at
http://jeb.biologists.org/lookup/doi/10.1242/jeb.183632.supplemental

References
Akaike, H. (1973). Information theory and extension of the maximum likelihood principle. In *Second International Symposium on Information Theory* (ed. B. N. Petrov and F. Csaki), pp. 267-281. Budapest: Akadémiai Kiadó.

Arey, L. B. and Crozier, W. J. (1919). The sensory responses of chiton. *J. Exp. Zool.* **29**, 157-260.

Batschelet, E. (1981). *Circular Statistics in Biology*. New York: Academic Press.

Baxter, J. M., Jones, A. M. and Sturrock, M. G. (1987). The infrastructure of aesthetes in *Tonicella marmorea* (Polyplacophora; Ischnochitonina) and a new functional hypothesis. *J. Zool.* **211**, 589-604.

Baxter, J. M., Sturrock, M. G. and Jones, A. M. (1990). The structure of the intrapigmented aesthetes and the properiostracum layer in *Callochiton achatinus* (Mollusca: Polyplacophora). *J. Zool.* **220**, 447-468.

Bechstedt, S., Lu, K. and Brouhard, G. J. (2014). Doublecortin recognizes the longitudinal curvature of the microtubule end and lattice. *Curr. Biol.* **24**, 2366-2375.

Blevins, E. and Johnsen, S. (2004). Spatial vision in the echinoid genus *Echinometra*. *J. Exp. Biol.* **207**, 4249-4253.

Bok, M. J., Bok, M. J., Capa, M., Capa, M., Nilsson, D.-E. and Nilsson, D.-E. (2016). Here, there and everywhere: the radiolar eyes of fan worms (Annelida, Sabellidae). *Integr. Comp. Biol.* **56**, 784-795.

Bok, M. J., Porter, M. L., ten Hove, H. A., Smith, R. and Nilsson, D.-E. (2017). Radiolar eyes of Serpulid worms (Annelida, Serpulidae): structures, function, and phototransduction. *Biol. Bull.* **233**, 39-57.

Boyle, P. R. (1969). Fine structure of the eyes of *Onithochiton neglectus* (Mollusca: Polyplacophora). *Z. Zellforsch Mikrosk Anat.* **102**, 313-332.

Boyle, P. R. (1972). The aesthetes of chitons. *Mar. Freshw. Behav. Physiol.* **1**, 171-184.

Burnham, K. P. and Anderson, D. R. (2004). Multimodel inference: understanding AIC and BIC in model selection. *Sociol. Methods Res.* **33**, 261-304.

Burnham, K. P., Anderson, D. R. and Huyvaert, K. P. (2011). AIC model selection and multimodel inference in behavioral ecology: some background, observations, and comparisons. *Behav. Ecol. Sociobiol.* **65**, 23-35.

Buschbeck, E., Ehmer, B. and Hoy, R. (1999). Chunk versus point sampling: visual imaging in a small insect. *Science* **286**, 1178-1180.

Chelazzi, G., Della Santina, P. and Parpagnoli, D. (1987). Trail following in the chiton *Acanthopleura gemmata*: operational and ecological problems. *Mar. Biol.* **95**, 539-545.

Chelazzi, G., Della Santina, P. and Parpagnoli, D. (1990). The role of trail following in the homing of intertidal chitons: a comparison between three *Acanthopleura* spp. *Mar. Biol.* **105**, 445-450.

Cronin, T. W., Johnsen, S., Marshall, N. J. and Warrant, E. J. (2014). *Visual Ecology.* Princeton: Princeton University Press.

Crozier, W. J. (1921). 'Homing' behavior in chiton. *Am. Nat.* **55**, 276-281.

Eernisse, D. J. and Reynolds, P. D. (1994). Microscopic anatomy of invertebrates. *Mollusca I* **5**, 55-110.

Fernandez, C. Z., Vendrasco, M. J. and Runnegar, B. (2007). Aesthete canal morphology in twelve species of chiton (Polyplacophora). *Veliger* **49**, 51-69.

Fitak, R. R. and Johnsen, S. (2017). Bringing the analysis of animal orientation data full circle: model-based approaches with maximum likelihood. *J. Exp. Biol.* **220**, 3878-3882.

Fordyce, D. and Cronin, T. W. (1993). Trilobite vision: a comparison of schizochroal and holochroal eyes with the compound eyes of modern arthropods. *Paleobiology* **19**, 288-303.

Garm, A. and Nilsson, D. E. (2014). Visual navigation in starfish: first evidence for the use of vision and eyes in starfish. *Proc. R. Soc. B* **281**, 20133011.

Haas, W. and Kriesten, K. (1978). Die Ästheten mit intrapigmentärem Schalenauge von *Chiton marmoratus* L. (Mollusca, Placophora). *Zoomorphologie* **90**, 253-268.

Hurvich, C. M. and Tsai, C.-L. (1989). Regression and time series model selection in small samples. *Biometrika* **76**, 297-307.

Labhart, T. and Nilsson, D.-E. (1995). The dorsal eye of the dragonfly Sympetrum: specializations for prey detection against the blue sky. *J. Comp. Physiol. A* **176**, 437-453.

Land, M. F. (1965). Image formation by a concave reflector in the eye of the scallop, *Pecten maximus. J. Physiol.* **179**, 138-153.

Land, M. F. and Nilsson, D.-E. (2002). *Animal Eyes.* Oxford, UK: Oxford University Press.

Li, L., Connors, M. J., Kolle, M., England, G. T., Speiser, D. I., Xiao, X., Aizenberg, J. and Ortiz, C. (2015). Multifunctionality of chiton biomineralized armor with an integrated visual system. *Science* **350**, 952-956.

Moseley, H. N. (1885). On the presence of eyes in the shells of certain chitonidae and on the structures of these organs. *Q. J. Microsc. Sci.* **25**, 37-60.

Nilsson, D. E. (1994). Eyes as optical alarm systems in fan worms and ark clams. *Phil. Trans. R. Soc. Lond. B* **346**, 195-212.

Nilsson, D.-E. (2009). The evolution of eyes and visually guided behaviour. *Philos. Trans. R. Soc. B Biol. Sci.* **364**, 2833-2847.

Nilsson, D.-E. (2013). Eye evolution and its functional basis. *Vis. Neurosci.* **30**, 5-20.

Nilsson, D.-E., Gislén, L., Coates, M. M., Skogh, C. and Garm, A. (2005). Advanced optics in a jellyfish eye. *Nature* **435**, 201-205.

Nilsson, D.-E. and Pelger, S. (1994). A pessimistic estimate of the time required for an eye to evolve. *Proc. R. Soc. B* **256**, 53-58.

Nowikoff, M. (1907). Uber die Rfickensinnesorgane der Placophoren nebst einigen Bemerkungen fiber die Schale derselben. *Z. Wiss. Zool.* **88**, 154-186.

Nowikoff, M. (1909). Uber die intrapigment~iren Augen der Placophoren. *Z. Wiss. Zool.* **93**, 668-680.

Oakley, T. H. and Speiser, D. I. (2015). How complexity originates: the evolution of animal eyes. *Annu. Rev. Ecol. Evol. Syst.* **46**, 237-260.

Okusu, A., Schwabe, E., Eernisse, D. J. and Giribet, G. (2003). Towards a phylogeny of chitons (Mollusca, Polyplacophora) based on combined analysis of five molecular loci. *Org. Divers. Evol.* **3**, 281-302.

Pairett, A. N. and Serb, J. M. (2013). De novo assembly and characterization of two transcriptomes reveal multiple light-mediated functions in the scallop eye (Bivalvia: Pectinidae). *PLoS ONE* **8**, e69852.

Palmer, B. A., Taylor, G. J., Brumfeld, V., Gur, D., Shemesh, M., Elad, N., Osherov, A., Oron, D., Weiner, S. and Addadi, L. (2017). The image-forming mirror in the eye of the scallop. *Science* **358**, 1172-1175.

Plachetzki, D. C. and Oakley, T. H. (2007). Key transitions during the evolution of animal phototransduction: novelty, 'tree-thinking', co-option, and co-duplication. *Integr. Comp. Biol.* **47**, 759-769.

Schindelin, J., Arganda-Carreras, I., Frise, E., Kaynig, V., Longair, M., Pietzsch, T., Preibisch, S., Rueden, C., Saalfeld, S., Schmid, B. et al. (2012). Fiji: an open-source platform for biological-image analysis. *Nat. Methods* **9**, 676-682.

Schnute, J. T. Groot, K. (1992). Statistical analysis of animal orientation data. *Anim. Behav.* **43**, 15-33.

Sirenko, B. (2006). New outlook on the system of chitons (Mollusca: Polyplacophora). *Venus* **65**, 27-49.

Speiser, D. I., Eernisse, D. J. and Johnsen, S. (2011). A chiton uses aragonite lenses to form images. *Curr. Biol.* **21**, 665-670.

Sumner-Rooney, L. and Sigwart, J. D. (2018). Do chitons have a brain? New evidence for diversity and complexity in the polyplacophoran central nervous system. *J. Morphol.* **29**, 751.

Sumner-Rooney, L. H., Murray, J. A., Cain, S. D. and Sigwart, J. D. (2014). Do chitons have a compass? Evidence for magnetic sensitivity in Polyplacophora. *J. Nat. Hist.* **48**, 3033-3045.

Sumner-Rooney, L., Rahman, I. A., Sigwart, J. D. and Ullrich-Lüter, E. (2018). Whole-body photoreceptor networks are independent of 'lenses' in brittle stars. *Proc. R. Soc. B* **285**, 20172590.

Tinevez, J.-Y., Perry, N., Schindelin, J., Hoopes, G. M., Reynolds, G. D., Laplantine, E., Bednarek, S. Y., Shorte, S. L. and Eliceiri, K. W. (2017). TrackMate: an open and extensible platform for single-particle tracking. *Methods* **115**, 80-90.

Ullrich-Lüter, E. M., Dupont, S., Arboleda, E., Hausen, H. and Arnone, M. I. (2011). Unique system of photoreceptors in sea urchin tube feet. *Proc. Natl Acad. Sci. USA* **108**, 8367-8372.

von Salvini-Plawen, L. and Mayr, E. (1977). On the evolution of photoreceptors and eyes. *Evol. Biol.* **10**, 207-263.

Wilkens, L. A. (1986). The visual system of the giant clam *Tridacna. Biol. Bull.* **170**, 393-408.